



Simple chalcones and *bis*-chalcones ethers as possible pleiotropic agents

Thalia Liargkova, Dimitra J. Hadjipavlou-Litina, Caterina Koukoulitsa, Efstathia Voulgari & Constantinos Avgoustakis

To cite this article: Thalia Liargkova, Dimitra J. Hadjipavlou-Litina, Caterina Koukoulitsa, Efstathia Voulgari & Constantinos Avgoustakis (2016) Simple chalcones and *bis*-chalcones ethers as possible pleiotropic agents, Journal of Enzyme Inhibition and Medicinal Chemistry, 31:2, 302-313, DOI: [10.3109/14756366.2015.1021253](https://doi.org/10.3109/14756366.2015.1021253)

To link to this article: <https://doi.org/10.3109/14756366.2015.1021253>



Published online: 23 Mar 2015.



Submit your article to this journal [↗](#)



Article views: 1726



View related articles [↗](#)



View Crossmark data [↗](#)



Citing articles: 11 View citing articles [↗](#)

RESEARCH ARTICLE

Simple chalcones and *bis*-chalcones ethers as possible pleiotropic agents

Thalia Liargkova¹, Dimitra J. Hadjipavlou-Litina¹, Caterina Koukoulitsa², Efstathia Voulgari³, and Constantinos Avgoustakis³

¹Department of Pharmaceutical Chemistry, School of Pharmacy, Aristotle University of Thessaloniki, Thessaloniki, Greece, ²Chemistry Department, University of Athens, Panepistimiopolis-Zografou, Greece, and ³Department of Pharmaceutical Technology and Pharmaceutical Analysis, School of Pharmacy, University of Patras, Rio Patras, Greece

Abstract

The synthesis, the antioxidative properties and the lipoxygenase (LOX) and acetylcholinesterase (AChE) inhibition of a number of 4-hydroxy-chalcones diversely substituted as well as of a series of *bis*-chalcones ether derivatives are reported. The chalcones derivatives were readily produced using a Claisen–Schmidt condensation in a ultra sound bath in good yields. The structures of the synthesized compounds were confirmed by spectral and elemental analysis. Their lipophilicity is experimentally determined by reversed-phase thin-layer chromatography method. Most of them are potent *in vitro* inhibitors of lipid peroxidation and of LOX. Compounds **b2** and **b3** were found to be the most potent LOX and AChE inhibitors among the tested derivatives with a significant anti-lipid peroxidation profile. The results led us to propose these enone derivatives as new multifunctional compounds against Alzheimer's disease. The results are discussed in terms of structural and physicochemical characteristics of the compounds. Moreover, the pharmacokinetic profile of these compounds was investigated using computational methods.

Introduction

Chalcones and their derivatives are natural or synthetic 1,3-diaryl-2-propenones that may exist in *cis* and *trans* isomeric forms, of which the latter is thermodynamically stable. Due to the enone system, such molecules present relatively low redox potentials and have a greater probability of undergoing electron transfer reactions. They possess an extended number of biological activities: regulate cholesterol levels, reduce blood pressure, regulate blood sugar, improve vision and memory, inhibit acetylcholinesterase, inhibit enzymes implicated in inflammation, reduce joint and muscular pains, enhance liver and kidney functions, aid sleep, prevent cancer, strengthen the immune system and beautify the skin and hair^{1,2}.

Hydroxyl chalcones embrace hydroxyl substitution, a key group to greatly enhance the antioxidant activity of chalcones, due to their conversion to phenoxyl radicals through the hydrogen atom transfer mechanism³. However, their effects on the central nervous system (CNS) are still largely unexplored.

Reactive oxygen species (ROS) have been shown as causative factors involved in many human degenerative diseases and antioxidants have been found to have some degree of preventive and therapeutic effects on these disorders^{4,5}. Evidence for involvement of free radicals in Alzheimer disease (AD) includes

Keywords

Acetylcholinesterase inhibitors, *bis*-chalcones, chalcones, lipoxygenase inhibitors, multitarget agents

History

Received 16 December 2014

Accepted 9 February 2015

Published online 23 March 2015

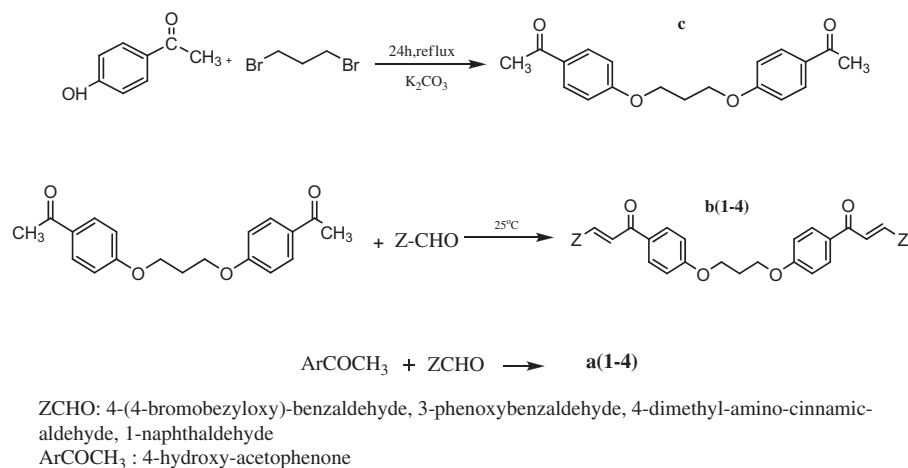
the presence of elevated levels of protein oxidation, lipid peroxidation products and oxidative damage to mitochondria in AD brain⁵. Antioxidants protect against the radicals and it is important to balance an enhanced radical production with a sufficient supply of antioxidants⁶. Increasing experimental evidence supports the view that inflammation-generated oxidative stress contributes to the lesions of AD⁷. According to the observed antioxidant activity of the majority of the examined chalcones, it has been concluded that are convenient templates when designing useful drugs in treating of Alzheimer's disease that involves ROS.

Acetylcholinesterase (AChE) is a carboxyl-esterase which terminates cholinergic neuro-transmission, by hydrolyzing neurotransmitter acetylcholine (ACh) in a synaptic cleft. Reversible AChE inhibition is implicated in a number of neurological disorders. It has been noticed that reduced AChE expression is a common feature of AD patients. However, higher levels of AChE are observed around β -amyloid plaques⁸. Thus AChE is another good target for AD treatment and it is generally accepted that AChE is associated with β -amyloid plaques. Accordingly, current approaches to AD treatment aim to an increase of ACh in the brain by AChE inhibitors⁹.

Lipoxygenases (LOXs) catalyze the first two steps in the metabolism of arachidonic acid to leukotrienes, important inflammatory mediators¹⁰. Recent findings show that the activation of brain LOXs is an early event in the pathogenesis of AD¹¹. Recently showed that AD brains had higher 5-LOX protein levels than did healthy controls¹². 5-Lipoxygenase (5-LOX) acts as a modulator of A β peptides formation *in vivo*. A new study points

Address for correspondence: Dr. Dimitra J. Hadjipavlou-Litina, Department of Pharmaceutical Chemistry, School of Pharmacy, Faculty of Health Sciences, Aristotle University of Thessaloniki, Thessaloniki 54124, Greece. E-mail: hadjipav@pharm.auth.gr

Figure 1. Synthetic procedures for the synthesis of chalcones **a1–a4**, of diether **c** and of *bis*-chalcones ethers **b1–b4**.



to a new role for 5-LOX in regulating endogenous tau metabolism in the CNS and supports the hypothesis that its pharmacologic inhibition could be beneficial for AD-related tau neuropathology¹³.

In the past years, targeted therapies toward a specific molecular target have been applied. Today, the diligence of inherent redundancy and robustness in many biological networks and pathways depicts that inhibiting a single target might fall short of producing the desired therapeutic effect^{14–16}. Multi-target drug strategies have emerged as a therapeutic approach to treat diseases that stem from a combination of factors. Multitarget therapeutic strategy can be used to inhibit two or more enzymes, act on an enzyme and a receptor, or affect an ion channel and a transporter¹⁷. Using this strategy, a single molecule hits multiple targets, which participate in pathways implicated to a given disease¹⁸. Therefore, it is evident that the treatment of AD could benefit from the use of multipotent drugs that present free radical scavenging, anti-inflammatory and AChE inhibitory activity.

It is in this context that herein we report the synthesis, the antioxidant as well as the anti-inflammatory and anti-AChE inhibitory activity of a number of 4-hydroxy-chalcones (Figure 1), diversely substituted as well as of a series of *bis*-chalcones combined together through an $-\text{OCH}_2\text{CH}_2\text{CH}_2\text{O}-$ linkage (Figure 1, structures **b1–b4**). The derived **b1–b4** molecules might be used as prodrugs, after an *in vivo* metabolism cascade, through which two smaller chalcones will be possible to be taken.

Nowadays in pharmaceutical research new challenges have been added for which additional considerations must be taken with respect to toxicological effects, as well as potential interactions with cytochrome P450, related to avoidance of Phase I metabolism.

Thus, as a contribution to the knowledge about the pharmacokinetic properties of the new compounds (simple/double chalcones) we will investigate their pharmacokinetic profile using the VolSurf procedure¹⁹.

Experimental

General

All starting materials and solvents were obtained from commercial sources and used without further purification. Melting points were determined in open glass capillaries using a Mel-TempII apparatus (Lab. Devices, Holliston, MA). UV-vis spectra were obtained on a Shimadzu UV-1700 PharmSpec (UVprobe Ver. 2.21) (Kanda-Nishikicho 1-chome, Tokyo, Japan). Infrared spectra (film as Nujol mulls or KBr) were recorded with a Shimadzu FT IR-8101 M (Kanda-Nishikicho 1-chome, Tokyo, Japan). The ¹H NMR spectra were recorded at 300 MHz on a Bruker AM 300

spectrometer (Bruker Analytische Messtechnik GmbH, Rheinstetten, Germany) in CDCl₃ or DMSO using tetramethylsilane (TMS) as an internal standard, unless otherwise stated. ¹³C NMR spectra were obtained at 75.5 MHz on a Bruker AM 300 spectrometer in CDCl₃ or DMSO solutions with TMS as internal reference unless otherwise stated. Mass spectra were determined on a Shimadzu LC-MS 2010 EV under electrospray ionization (ESI) conditions [MS (ESI)] (Shimadzu Scientific Instruments, Inc., Columbia, MD). Elemental analyses were obtained in an acceptable range ($\pm 0.4\%$) in a Perkin-Elmer 240 B CHN analyzer (Perkin-Elmer Corporation Ltd., Lane Beaconsfield, Bucks, UK). Reactions were monitored by thin-layer chromatography (TLC) by Fluka, on aluminum cards precoated with 0.2 mm of silica gel and fluorescent indicator. For reversed-phase TLC (RP-TLC) silica gel 60 Merck F₂₅₄ plates were used. Ultra sound bath (US-bath) Bandelin Sonorex Typ: RK100H was used. Azobis(2-aminodipropyl) dihydrochloride (AAPH), 1,1-diphenyl-picrylhydrazyl (DPPH), nordihydroguaretic acid (NDGA) and Trolox were purchased from the Aldrich Chemical Co. (Milwaukee, WI). Soybean LOX, linoleic acid sodium salt were obtained from Sigma Chemical Co. (St. Louis, MO). For the *in vitro* tests a UV-1700. PharmSpec Shimadzu UV-Vis double beam spectrophotometer was used.

Synthesis

General method for the synthesis of chalcones **a** (1–4)

A modified Claisen-Schmidt condensation was performed between 4-hydroxy acetophenone and the suitable substituted aryl aldehyde at a molar ratio 1:1 in absolute ethanol (10 mL). Three milliliters aqueous KOH (20%) was added. The mixture was stirred at room temperature in a US-bath the end of the reaction was monitored by TLC. The mixture was neutralized treated with aqueous HCl 10%. The precipitate was either filtered and washed with cold water or extracted with CHCl₃ (30 mL \times 3). The combined organic layers were washed with water and brine and dried under anhydrous MgSO₄. The product was evaporated to dryness and purified by recrystallization from a proper solvent.

(i) A modification of the above method was performed, in which the mixture of the reactants was heated in a microwave oven for 15 min (50 W, 60 °C). Under these experimental conditions, we have synthesized the known **a2** chalcone²⁰.

3-(4-((4-Bromobenzyl)oxy)phenyl)-1-(4-hydroxyphenyl)prop-2-en-1-one (a1). 76% yield, yellow solid, m.p. 117–119 °C. *R*_f: 0.47 (2:1, hexane/acetone). Recrystallized from ethanol, IR (KBr): 1710, 1610 cm⁻¹; ¹H NMR (CDCl₃): δ 5.08 (d, 2H), 6.90 (d, 1H)

7.01 (d, 2H), 7.28–7.31 (m, 5H), 7.51–7.72 (m, 3H), 7.83 (m, 2H), 7.97 (d, 1H, $J = 9$ Hz), 9.89 (s, 1H); ^{13}C NMR (CDCl_3): δ 40, 76.50, 77, 77.40, 110.6, 110.95, 111.70, 117.97, 118.4, 118.85, 121.74, 123.75, 130.44, 130.67, 132, 136.4, 152.37, 153.89, 190.28. Anal. Calcd for $\text{C}_{22}\text{H}_{17}\text{BrO}_3$: C, 64.56; H, 4.19. Found: C, 64.35; H, 4.07.

1-(4-Hydroxyphenyl)-3-(3-phenoxyphenyl)prop-2-en-1-one (a2). The modified (i) synthetic method was used. The analytical data as well as the spectra analysis were in agreement to the corresponding given in literature²⁰.

5-(4-(Dimethylamino)phenyl)-1-(4-hydroxyphenyl)penta-2,4-dien-1-one (a3). 79% yield, dark brown solid, m.p. 220–222 °C. R_f : 0.55, 0.55 (2:1, hexane/acetone). Recrystallized from ethanol, IR (KBr): 1710, 1620 cm^{-1} ; ^1H NMR (CDCl_3): δ 2.61–3.26 (m, 6H), 6.51–7.95 (m, 12H), 12.3 (s, 1H); ^{13}C NMR (CDCl_3): δ 77.42, 125.43, 126.95, 127.27, 128.56, 128.82, 129.21, 132.64, 141.89, 144.84, 160.82, 163.37, 163.60, 187.20; MS (ESI): 293 $[\text{M}-1]^+$, 293 $[\text{M}+\text{CH}_3\text{CH}_2\text{OH}+\text{Na}]^+$. Anal. Calcd for $\text{C}_{19}\text{H}_{19}\text{NO}_2$: C, 77.79; H, 6.53; N, 4.77. Found: C, 77.86; H, 6.77; N, 4.85.

1-(4-Hydroxyphenyl)-3-(naphthalen-1-yl)prop-2-en-1-one (a4). see Ref²¹.

Synthesis of 1,1'-((propane-1,3-diylbis(oxy))bis(4,1-phenylene)) diethanone (c)

4-Hydroxy acetophenone and 1,3-dibromopropane in molar ratio 2:1 was diluted in 50 mL acetone. Anhydrous K_2CO_3 was added and the mixture was refluxed for approximately 18 h. The reaction was completed judged by the negative alcoholic ferric chloride (3%) test. The mixture was evaporated to dryness. The solid was treated with water, filtered of and recrystallized from absolute ethanol.

90% yield, white crystals solid, m.p. 115–117 °C. R_f : 0.53 (2 hexane:1 acetone), IR (KBr): 1750, 1670 cm^{-1} ; ^1H NMR (CDCl_3): δ 2.27–2.35 (m, 2H), 2.54 (br, 6H), 4.21–4.25 (m, 4H), 6.87–6.96 (m, 4H), 7.91–7.94 (m, 4H); ^{13}C NMR (CDCl_3): δ 26.3, 26.2, 29.1, 64.5, 65, 114.2, 130.6, 130.6, 136.4, 162.7, 196.6, 196.6. Anal. Calcd for $\text{C}_{19}\text{H}_{20}\text{O}_4$: C, 73.06; H, 6.45. Found: C, 72.98; H, 6.37.

Synthesis of etherified double chalcones b (I–4)

General synthetic method. A Claisen–Schmidt condensation was performed between (1,1'-((propane-1,3-diylbis(oxy))bis(4,1-phenylene))diethanone) and the appropriate substituted aromatic aldehyde at a molar ratio 1:2 in absolute ethanol (10 mL)²². Three milliliters aqueous KOH (20%) was added. The mixture was stirred at room temperature in a US-bath. The end of the reaction was monitored by TLC. After the completion of the reaction the mixture was neutralized treated with aqueous HCl 10%. The precipitate was either filtered and washed with cold water or extracted with CHCl_3 (30 mL \times 3). The combined organic layers were washed with water and brine and dried under anhydrous MgSO_4 . The product was evaporated to dryness and purified by recrystallization from a proper solvent.

1,1'-((Propane-1,3-diylbis(oxy))bis(4,1-phenylene))bis(3-(4-(4-bromobenzyl)oxy)phenyl)prop-2-en-1-one (b1). 89% yield, light yellow solid, m.p. 197–199 °C. R_f : 0.5(2:1, hexane/acetone). Recrystallized from acetone, IR (KBr): 1660, 1630 cm^{-1} ; ^1H NMR (CDCl_3): δ 2.31–2.35 (m, 2H), 5.06 (s, 4H), 4.24–4.28 (m, 4H), 6.93–7.05 (m, 4H), 7.26–7.31 (m, 8H), 7.38–7.43 (m, 4H), 7.755 (d, 2H), 8.015 (s, 4H), 7.36 (s, 2H), 7.43–7.66 (m, 4H); ^{13}C NMR (CDCl_3): δ 45.6, 64.5, 69.4, 66.6, 77, 77.4, 114.3, 115, 120, 122, 128, 129, 130, 130.7, 132, 135, 135.6, 143.7, 151.6, 160.4,

188.7, 188.7; MS (ESI): 891 $[\text{M}+\text{CH}_3\text{OH}+1]^+$. Anal. Calcd for $\text{C}_{47}\text{H}_{38}\text{Br}_2\text{O}_6$: C, 65.75; H, 4.46. Found: C, 65.92; H, 4.34.

1,1'-((Propane-1,3-diylbis(oxy))bis(4,1-phenylene))bis(3-(3-phenoxyphenyl)prop-2-en-1-one) (b2). 72% yield, yellow solid, m.p. 172–174 °C. R_f : 0.68 (2:1, hexane/acetone). Recrystallized from ethanol, IR (KBr): 1680, 1650 cm^{-1} ; ^1H NMR (CDCl_3): δ 2.16–2.54 (m, 2H), 4.24–4.28 (m, 4H), 6.93–7.22 (m, 12H), 7.28–7.56 (m, 8H), 7.62–7.69 (m, 4H), 7.75–7.91 (m, 2H), 7.97–8.07 (m, 4H); ^{13}C NMR (CDCl_3): δ 29, 54, 54.6, 64.6, 114.4, 118.1, 119, 120.6, 122.7, 123.4, 126, 129.9, 130.2, 130.9, 131.2, 137, 143, 153, 156.9, 157.9, 162.7, 188.5. Anal. Calcd for $\text{C}_{45}\text{H}_{36}\text{O}_6$: C, 80.34; H, 5.39. Found: C, 80.34; H, 5.43.

1,1'-((propane-1,3-diylbis(oxy))bis(4,1-phenylene))bis(5-(4-(dimethylamino)phenyl)penta-2,4-dien-1-one) (b3). 79% yield, dark brown solid, m.p. 156–158 °C. R_f : 0.55, 0.62 (2:1, hexane/acetone). Recrystallized from ethanol, IR (KBr): 1710, 1670 cm^{-1} ; ^1H NMR (CDCl_3): δ 2.29–2.54 (s, 2H), 2.99–3.08 (br, 12H), 4.22–4.26 (m, 4H), 6.68–6.94 (m, 10H), 7.31–7.56 (m, 2H), 7.59–7.64 (m, 2H), 7.91–7.98 (m, 10H); ^{13}C NMR (CDCl_3): δ 29.4, 64, 100.4, 109, 11.2, 112.4, 114.2, 118.3, 121.5, 124.5, 128.8, 130.5, 130.6, 131.9, 135.6, 141.6, 145.5, 158.3, 186.2. Anal. Calcd for $\text{C}_{41}\text{H}_{42}\text{N}_2\text{O}_4$: C, 78.57; H, 6.75; N, 4.47. Found: C, 78.4; H, 7.03; N, 4.10.

1,1'-((Propane-1,3-diylbis(oxy))bis(4,1-phenylene))bis(3-(naphthalen-1-yl)prop-2-en-1-one) (b4). 74% yield, yellow solid, m.p. 167–168 °C. R_f : 0.64 (2:1, hexane/acetone). Recrystallized from petroleum ether:ethylacetate, IR (KBr): 1680, 1630 cm^{-1} ; ^1H NMR (CDCl_3): δ 2.31–2.54 (m, 2H), 4.2–4.28 (m, 4H), 7.0–7.03 (m, 4H), 7.48–7.64 (m, 8H), 7.86–7.92 (m, 8H), 8.07–8.27 (m, 2H), 8.255 (d, 2H), 8.64 (d, 2H); ^{13}C NMR (CDCl_3): δ 29.6, 64, 76, 114.4, 117.1, 123.6, 124.7, 124.9, 125.4, 126.3, 126.9, 128.7, 130.6, 130.9, 131.3, 131.8, 132.7, 133.8, 141, 162.7, 18.5; MS (ESI): 611 $[\text{M}+\text{Na}]^+$. Anal. Calcd for $\text{C}_{41}\text{H}_{32}\text{O}_4$: C, 83.65; H, 5.48. Found: C, 83.63; H, 5.87.

Physicochemical studies

Experimental determination of lipophilicity as R_M values

RPTLC was performed on silica gel plates impregnated with 55% (v/v) liquid paraffin in light petroleum ether. The mobile phase was a methanol/water mixture (70/30, v/v). The plates were developed in closed chromatography tanks saturated with the mobile phase at 24 °C. Spots were detected under UV light or by iodine vapors. R_M values were determined from the corresponding R_f values (from 10 individual measurements) using the equation $R_M = \log[(1/R_f) - 1]$ ²³.

Theoretically calculated values of lipophilicity as clog P

Lipophilicity was theoretically calculated as clog P values in n -octanol-buffer by CLOGP Programme of Biobyte Corp.²⁴.

Biological experiments

General methods

Each *in vitro* experiment was performed at least in triplicate and the standard deviation of absorbance was less than 10% of the mean.

In vitro assays

Determination of the reducing activity of the stable radical 1,1-diphenyl-picrylhydrazyl. To a solution of 1,1-diphenyl-picrylhydrazyl (DPPH) in absolute ethanol an equal volume of

the compounds dissolved in DMSO was added. A stock solution (10 mM) of the compounds was used. The concentrations of the final solutions of the compounds were 100 μ M. After 20 and 60 min at room temperature the absorbance was recorded at 517 nm²⁵.

Inhibition of linoleic acid peroxidation. Production of conjugated diene hydroperoxide by oxidation of sodium linoleate in an aqueous dispersion was monitored at 234 nm²⁶. AAPH is used as a free radical initiator. Ten microliters of the 16 mM sodium linoleate solution was added to the UV cuvette containing 0.93 mL of 0.05 M phosphate buffer, pH 7.4 prethermostated at 37 °C. The oxidation reaction was initiated at 37 °C under air by the addition of 50 μ L of 40 mM AAPH solution. Oxidation was carried out in the presence of aliquots (10 μ L) in the assay without antioxidant. Lipid oxidation was measured in the presence of the same level of DMSO. The rate of oxidation at 37 °C was monitored by recording the increase in absorption at 234 nm caused by conjugated diene hydroperoxides and compared with the appropriate standard trolox.

Soybean LOX inhibition study in vitro. *In vitro* study was evaluated as reported previously²⁵. The tested compounds dissolved in DMSO were incubated at room temperature with sodium linoleate (100 μ M) and 0.2 mL of enzyme solution ($1/9 \times 10^{-4}$ w/v in saline). The conversion of sodium linoleate to 13-hydroperoxylinoic acid at 234 nm was recorded and compared with the appropriate standard inhibitor (NDGA). Several concentrations were used for the determination of IC₅₀ values.

Glutathione conjugation. Stock solutions of the compounds were prepared in water using phosphate buffer solution (PBS) pH 7.4 and in order to achieve dissolution the solvent contained approximately 10% DMSO. The concentrations of the solutions were chosen so that the absorption maxima were between 0.5 and 1. The test compounds are incubated for 24 h at 37 °C and their UV spectra were recorded. All determinations were carried out in duplicate. The error limits of the ϵ values were approximately 2%. The experiment was repeated in the presence of GSH using thiol/test compound, 2/1 and incubation at 37 °C for 24 h and their UV spectra were recorded^{25,27}.

Inhibition of acetylcholinesterase in vitro²⁸. A modified Ellman procedure was followed. The inhibitory activity was measured by the change in absorbance at 412 nm. The assay uses the thiol ester acetylthiocholine (0.01 M), which is hydrolyzed by AChE (3.5 U/mL) to produce thiocholine and acetate. The thiocholine reduces DTNB (0.01 M in phosphate 0.1 M pH 7) liberating nitrobenzoate, which absorbs at 412 nm. A 10-mM stock solution of the compounds in DMSO was used, from which several dilutions were made for the determination of IC₅₀ values. The experiment was performed in phosphate buffer pH 8 (0.1 M). As a standard inhibitor physostigmine was used.

Computational methods

The structures **a1–a4** and **b1–b4** were generated using SYBYL²⁹ Sybyl molecular modeling package running on a Linux operating system, and their energy were minimized using the Powell method with a convergent criterion provided by the Tripos force field³⁰.

Prediction of the site of metabolism. MetaSite^{31,32} is a computational procedure specifically designed to predict the site of metabolism of compounds, which metabolized by several cytochromes (CYP1A1, CYP1A2, CYP2C9, CYP2B6, CYP2C19, CYP2D6, CYP2E1 and CYP3A4). The prediction of the site of

metabolism is based on the hypothesis that the distance between the reactive center on the protein (oxygen atom attached to the iron atom) and the interaction points in the protein cavity (GRID-MIF) should correlate to the distance between the reactive center of the molecule (i.e. hydrogen atoms and heteroatoms positions) and the position of the different atom types in the molecule. This detailed information can be used by chemists in an early absorption, distribution, metabolism, and elimination (ADME) phase to increase the metabolic stability of drug candidates or to select appropriate chemical modifications leading to a better pharmacokinetics and metabolic profile.

Prediction of BBB permeation and Caco-2 permeability. Blood–brain barrier (BBB)³³ permeation and Caco-2 cell permeability³⁴ of the studied compounds were predicted using VolSurf (version 4, version 4.1.4, Molecular Discovery Ltd., 2005; www.moldiscovery.com). We used the probes water (OH2), hydrophobic (DRY) and H-bonding carbonyl (O) to generate the 3D interaction energies and a grid space of 0.5 Å.

Evaluation of the cytotoxicity

L929 mouse fibroblasts cells were cultured in EMEM supplemented with 10% horse serum, 2 mM L-glutamine, 1 mM sodium pyruvate, 0.1 mM nonessential amino acids, 1.5 g/L sodium bicarbonate and 100 μ g/mL penicillin–streptomycin at 37 °C in a humidified atmosphere with 5% CO₂³⁵.

L929 cells were plated into 24-well plates at a density 5×10^4 cells/well and allowed to attach and grow for 24 h. The supernatant in each well then replaced with medium containing various concentrations of **a1**, **a2**, **a3**, **a4**, **c**, **b1**, **b2**, **b3** and **b4**: 1, 10, 20, 50 and 100 μ M. After 24 h incubation, the supernatant was removed and the cells were washed with PBS. The cells were detached with 0.25% trypsin, transferred to FACS tubes and then centrifuged (1600 rpm for 5 min) and the pellet washed with PBS. After washing, the cells in the pellet were incubated with 5 μ L propidium iodide (PI) solution (1 mg/mL) for 1 min.

The PI fluorescence (cell death) was determined with flow cytometry, FACS Calibur, Coulter Epics XL-MCL. The analysis of flow cytometry data was performed with WinMDI analysis program.

Results and discussion

Chemistry

The chalcone analogs **a** (**1–4**) and **b** (**1–4**) were successfully synthesized via Claisen–Schmidt condensation, using KOH as a catalyst in a US-bath. In our study, we found that the use of the US-bath greatly affected the reactivity as well as the yields. The synthesis of the chalcones **a** (**1–4**), of bis-chalcones **b** (**1–4**) and of the diether **c**, is shown in Figure 2. Chalcones **a2** and **a4** have been synthesized earlier by other investigators^{20,21}. Herein we used modified synthetic procedures with better yields and less reaction time. In all cases, the use of US-bath diminished the reaction time and enhanced yields. Their structural characteristics and physicochemical properties were in agreement with the literature.

The structures of the new derivatives (**a1**, **a3**, **c**, **b1–b4**) have been analyzed and (Figure 2) confirmed spectroscopically [IR, ¹H NMR, ¹³C NMR, MS (ESI)] and by their elemental analysis. All the chalcones (**a** and **b**) present the characteristic absorption in the IR (nujol) (cm⁻¹ 3200 (O–H), 1720 (C=O), 1625 (C=C)). ¹H NMR spectroscopy did not succeed to delineate the (*E*)/(*Z*) structure. Previous findings²² supported the (*E*) conformation. The products were obtained in good yields (over 70%). The physical data of the synthesized compounds are given in details in the experimental session.

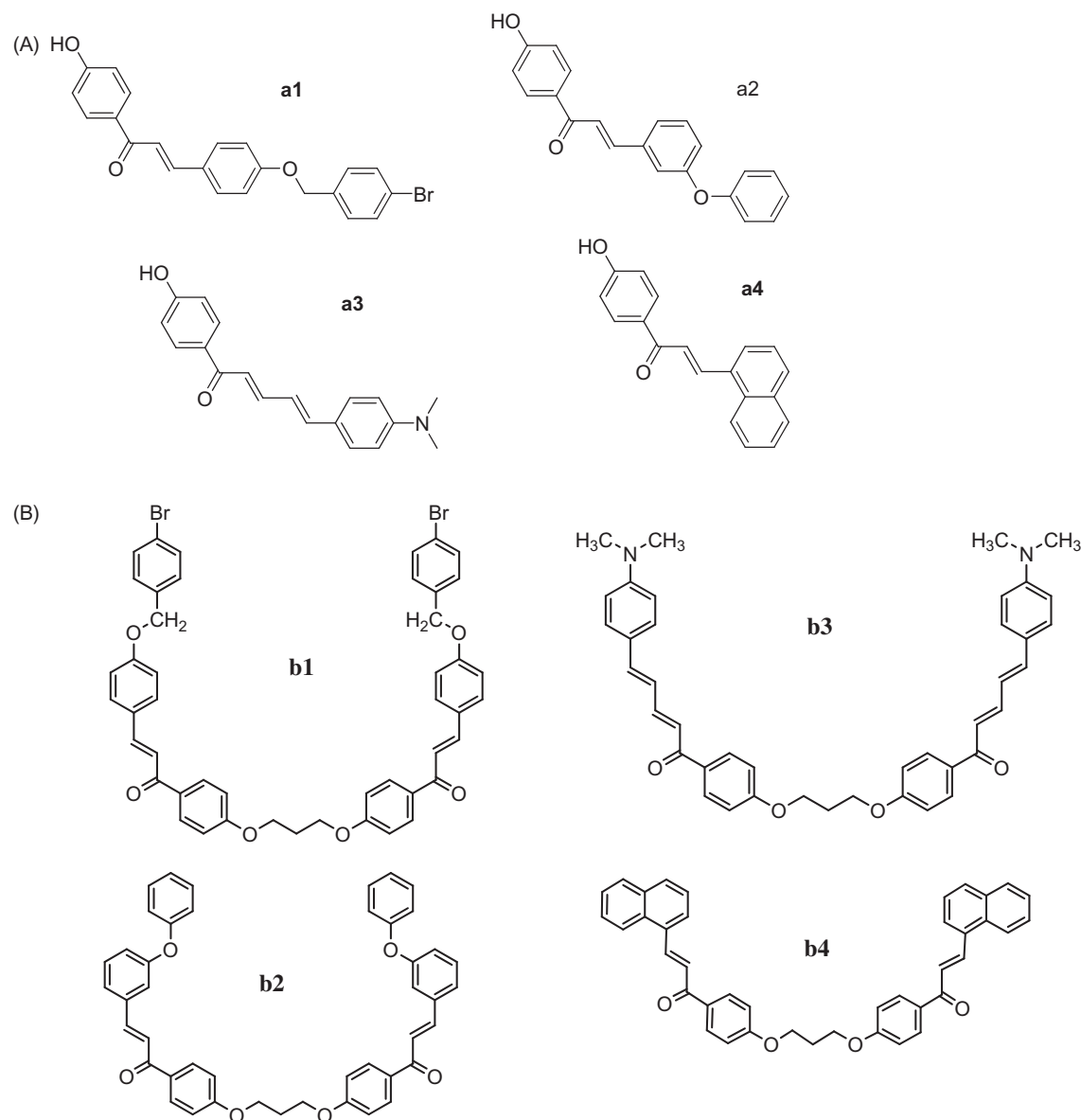


Figure 2. (A) 4-Hydroxy-substituted chalcones **a** (1–4). (B) Bis-chalcones etherified derivatives **b** (1–4).

Physicochemical studies

Lipophilicity is a significant physicochemical property determining distribution, bioavailability, metabolic activity and elimination. Thus, we tried to determine experimentally their lipophilicity from RPTLC method as R_M values and to compare them with the corresponding theoretically calculated $\log P$ values²⁴ in *n*-octanol-buffer. This is considered to be a reliable, fast and convenient method for expressing lipophilicity²³. Apart from the important role of lipophilicity for the kinetics of biologically active compounds, antioxidants of hydrophilic or lipophilic character are both needed to act as radical scavengers in the aqueous phase or as chain-breaking antioxidants in biological membranes.

From our results (Table 1), it can be concluded that R_M values could be used as a successful relative measure of the overall lipophilic/hydrophilic balance of these molecules.

$$R_M = 0.246(0.133) \log P - 1.200(0.782), \quad (1)$$

$$N = 7, \quad R = 0.906, \quad R^2 = 0.820, \quad S = 0.270, \\ F_{1,5} = 22.78, \quad \alpha = 0.01.$$

Table 1. Lipophilicity values: (i) theoretically calculated as $\log P$ and (ii) experimentally determined as R_M .

Compounds	$\log P$	$R_M (\pm SD)$
a1	6.05	0.34 (0.003)
a2	5.60	0.36 (0.001)
a3	3.66	−0.69 (0.005)
a4	4.67	−0.26 (0.002)
c	3.68	−0.23 (0.002)
b1	12.16	0.23 (0.02)
b2	11.07	−0.68 (0.005)
b3	9.00	0.89 (0.005)
b4	9.23	0.77 (0.007)

R_M values were significantly correlated to the theoretical $\log P$ values. Two derivatives have been omitted from this correlation (**b1** and **b2**). Their $\log P$ values were high (unrealistic range of lipophilicity in nature). This conclusion was supported by the statistical data given with Equation (1) (e.g. correlation coefficients, F values).

Table 2. Interaction–RA% with DPPH (RA%); % inhibition of lipid peroxidation (AAPH%); *in vitro* inhibition of soybean LOX (IC₅₀ or %); *in vitro* inhibition of AChE (IC₅₀ or %).

Compounds	RA% 100 μ M 20 min	RA% 100 μ M 60 min	AAPH% at 100 μ M	IC ₅₀ or %LOX inh. at 100 μ M	IC ₅₀ or % AChE at 100 μ M
a1	1.0	6.0	94.0	14.0%	7.0%
a2	3.0	4.0	94.0	10.0%	26.0%
a3	18.0	17.0	40.0	100 μ M	100.0 μ M
a4	7.0	3.0	96.0	44.0%	25.0%
c	No	No	20.0	No	13.0%
b1	36.0	55.0	51.0	40.0%	23.0%
b2	No	8.0	78.0	55.0 μ M	49.0 μ M
b3	17.0	14.0	100.0	56.0 μ M	52.0 μ M
b4	19.0	50.0	100.0	55.0 μ M	100.0 μ M
Trolox			63.0		
Physostigmin					0.05 μ M*
NDGA	81.0	83.0		28 mM	

No, no activity under the reported experimental conditions; confidence limits less than $\pm 10\%$. *76% at 100 μ M.

Calculation methods

Some physicochemical properties such as the energy values of the lowest and highest unoccupied molecular orbital (E_{LUMO} and E_{HOMO}) of the chalcones, the electrostatic potential and so on were calculated by the program Spartan v. 5.1.3 (Wavefunction Inc.) on energy minimized structures. These results were subjected to a multivariate analysis in order to describe better the activity of the compounds in terms of quantitative structure activity relationships.

Biological evaluation

The obtained products were evaluated as potential antioxidants/anti-inflammatory agents and inhibitors of AChE. The anti-inflammatory activity of the synthesised compounds was tested as *in vitro* inhibition of LOX activity. Their antioxidant potential was evaluated by the offered inhibition of lipid peroxidation, and by their interaction with 1,1-diphenyl-2-picrylhydrazyl stable radical.

The antioxidant ability of a compound must be evaluated in a variety of milieus. In this way, factors such as solubility or steric hindrance which may be of overriding importance in one environment in another can be varied. Thus, we have used two different types of assays to measure *in vitro* antioxidant activity: (a) the interaction with the stable free radical DPPH and (b) the interaction with the water-soluble azo compound AAPH.

Both require a spectrophotometric measurement and a certain reaction time in order to obtain reproducible results³⁶. The DPPH method is described as a simple, rapid and convenient method independent of sample polarity for screening many samples for radical scavenging activity³⁷. The use of the free radical reactions initiator AAPH is recommended as more appropriate for measuring radical-scavenging activity *in vitro*, because the activity of the peroxy radicals produced by the action of AAPH shows a greater similarity to cellular activities such as lipid peroxidation²⁶.

The interaction/reducing activity (RA) of the examined compounds with the stable free radical DPPH is shown in Table 2. This interaction, which indicates their radical scavenging ability in an iron-free system, was measured at 100 μ M (20/60 min). For the sake of comparison, already established RA% values for the intermediate molecule **c** were included in the table.

In the DPPH assay, the dominant chemical reaction involved is the reduction of the DPPH radical by an electron transfer from the antioxidant³⁸. Particularly effective such antioxidants are the phenoxide anions from phenolic compounds like catechol and derivatives, such as NDGA. Regarding their ability to reduce

DPPH, the simple 4-hydroxy chalcones **a** (**1–4**) did not reduce DPPH. The decrease/absence of the RA seems to be correlated to steric hindrance. The *bis*-chalcones **b1** and **b4** showed interesting reducing ability (50–55%), compared to the reference compound NDGA (83%). The highest RA (55%) is observed by **b1** after 60 min. Although in most cases the interaction remained constant after 60 min, an increase was observed for *bis*-chalcones **b1** and **b4**. Taking into consideration the fact that **a** (**1–4**), present very low, if any, RA on DPPH, it is apparent that *bis*-chalcones **b1** and **b4** do lead to compounds with improved antioxidant activity compared to the simpler molecules (**a1** and **a4**). The ether linkage does not seem to offer to the interaction with DPPH because the simple intermediate **c** does not show any interaction with DPPH at 100 μ M. Taking under consideration the calculated physicochemical properties of the molecules, such as the energy values of the lowest and highest unoccupied molecular orbital (E_{LUMO} and E_{HOMO}), the electrostatic potential, and so on (Table 3), it seems that their reducing ability RA is mainly correlated with E_{HOMO} . Thus, **b1** and **b4** with the lowest E_{HOMO} values (-0.2286 and -0.214549) are the most potent.

The low interaction values observed with **b2** and **b3** *bis*-chalcones can be attributed to the absence of easily oxidizable functionalities like the ones (two catechol subunits) present in NDGA as well as to their E_{HOMO} values. Lipophilicity does not seem to play an important role.

In the AAPH assay, the highly reactive alkylperoxyl radicals are intercepted mainly by a hydrogen atom transfer from the antioxidant. Therefore, particularly effective hydrogen atom transfer agents are compounds with high hydrogen atom donating ability, that is compounds with low heteroatom-H bond dissociation energies and/or compounds from which hydrogen abstraction leads to sterically hindered radicals as well as compounds from which abstraction of hydrogen leads to C-centered radicals stabilized by resonance.

Perusal of the percentage anti-lipid peroxidation activity (AAPH%) in Table 2 showed high inhibition of lipid peroxidation, higher than trolox (63%), with the exception of **a3** (40%) and **b1** (51%). Judging separately the anti-lipid peroxidation activity of the two chalcones groups, it seems that within the simple chalcones (**a1–a4**), low lipophilicity (as $\log P$ value), led to low inhibitory ability (**a3**=40%, $\log P$ = 3.66). The *bis*-chalcones **b1** and **b2** were found less active compared to the corresponding simple chalcones **a1** and **a2** due to their stereochemistry and bulk. Among the *bis*-chalcones (**b1–b4**) the antioxidant activity was found to be higher for **b3/b4** chalcones, which presented the lower $\log P$ values (9.0–9.23) within the

Table 3. Physicochemical properties calculated by the program Spartan v. 5.1.3.

Compounds	MW	Volume As	Surface area	Dipole (Debye)	Sm ² total energy (kcal/m)
c	626.79	750.99	760.47	1.667435	
b1	858.62	860.24	855.76	3.324089	−24.44
b2	672.77	769.3	757.36	2.256212	−8.32
b3	626.79	750.26	756.21	1.60489	31.65
b4	464.56	544.35	546.24	0.238953	−38.39
a1	409.27	406.73	408.65	3.59584	−26.11
a2	316.35	362.75	317.24	2.273257	−20.39
a3	293.36	353.57	372.09	3.841782	−7.89
a4	274.31	316.89	327.46	1.974221	−5.45
	<i>E</i> _{HOMO}	<i>E</i> _{LUMO}	<i>E</i> (bandgap)	Elpotmin	Elpotmax
c	−0.265419	0.058602	0.324021	−51.9398	36.8835
b1	−0.22806	0.19129	0.41935	−41.5485	27.0606
b2	−0.244199	0.180312	0.424511	−38.5631	21.6093
b3	−0.268259	0.062454	0.330714	−57.3943	28.5348
b4	−0.214549	0.187093	0.401642	−38.253	18.1817
a1	−0.305302	0.0878556	0.393158	−55.138	53.9305
a2	−0.309998	0.081237	0.391235	−47.1648	76.9638
a3	−0.268314	0.06715	0.335464	−50.8953	73.2086
a4	−0.277466	0.068504	0.34597	−47.4675	75.1948

subgroup. The intermediate **c** presents low anti-lipid peroxidation ability.

Regression analyses including all the values of anti-lipid peroxidation (AAPH %) revealed that lipophilicity, as *R*_M values (experimentally determined lipophilicity), was the main physicochemical parameter influencing their inhibitory activity and this was supported by the statistical data presented within Equation (2).

$$\log \text{AAPH}\% = 0.383(0.351)R_M + 1.701(0.197), \quad (2)$$

$$N = 7, \quad R = 0.782, \quad R^2 = 0.612, \quad S = 0.184,$$

$$F_{1,5} = 7.89, \quad \alpha = 0.01.$$

Two *bis*-chalcones **b1** and **b2** did not follow this model of activity. Their activity was not correlated with lipophilicity. Both present unrealistic high *clog P* values.

In an attempt to investigate the mechanism of the anti-inflammatory activity of chalcones and *bis*-chalcones, their *in vitro* effect on soybean LOX was examined. Soybean LOXs convert linoleic acid to 13-hydroperoxylinoleic acid, producing a conjugated diene that absorbs at 234 nm. It has been shown that inhibition of soybean LOX activity by nonsteroidal anti-inflammatory agents is qualitatively similar to their inhibition of the rat mast cell LOX and may be used as a simple qualitative screen for such activity³⁹.

NDGA, a known inhibitor of soybean LOX, has been used as a reference compound (IC₅₀ 28 mM/93% at 100 μM).

Perusal of the %/IC₅₀s inhibition values (Table 2) showed that the most potent, and almost equipotent, inhibitors were *bis*-chalcones **b2**, **b3** and **b4** with the exception of **b1**. The intermediate ether **c** was found inactive whereas simple 4-hydroxy chalcones **a1**, **a2** and **a4** exhibited activities in the range 10–44% at 100 μM. It is important to be noticed that the transformation of **a3** to the *bis*-chalcone ether **b3** led to a more potent derivative (IC₅₀ = 56 μM). Lipophilicity was referred as an important physicochemical property for LOX inhibition⁴⁰. This physicochemical property could explain the increase of anti-LOX activity in **b3** (*clog P* values for **a3** = 3.66, whereas **b3** = 9.00). For the same reason **b1**, **2** and **4** exhibited higher activities (in terms of % or IC₅₀ values) than the simple chalcones.

In an attempt to get deeper into the implicated physicochemical properties, we decided to analyze the % inhibition values induced by the compounds at 100 μM (LOX %, Table 2) instead of the IC₅₀ values, due to the small number of data. We found that *E*_{HOMO}, the energy value of the highest unoccupied molecular orbital, was the main physicochemical parameter influencing their inhibitory activity (Equation 3). Again *bis*-chalcones **b1** and **b2** were rejected from correlation (3). Their *E*_{HOMO} (Table 3) values did not present great differences.

$$\log \% \text{LOX} = 10.442(6.269)E_{\text{HOMO}} + 4.435(1.687), \quad (3)$$

$$N = 7, \quad R = 0.886, \quad R^2 = 0.786, \quad S = 0.206,$$

$$F_{1,5} = 18.37, \quad \alpha = 0.01.$$

There is no universally accepted approach to evaluate the relative potency of different substances to cause LOX inhibition. However, most of the LOX inhibitors are antioxidants or free radical scavengers⁴⁰. Herein, the results from the anti-lipid peroxidation activity studies support the anti-LOX activity for the *bis*-chalcones **b1–b4**.

We investigated *in vitro* the inhibitory activity of **a** and **b** on AChE activity, using acetylthiocholine as substrate²⁸. The applied method is based on the colorimetric determination of thiocholine produced through the catalytic activity of AChE, by its reaction with dithio-*bis*nitrobenzoic acid. The potential of these compounds to act as AChE inhibitors can be considered beneficial for their prospective nootropic action and may contribute to the mechanisms of action of reported structurally related hydroxyl chalcones⁴¹.

Bis-chalcone derivatives **b2** and **b3** were found to present significant and close IC₅₀ values (49/52 μM) followed by **b4** with the exception of **b1**. The simple **a** chalcones were found less active with a % inhibition range from 7% to 26% (Table 2). Only **a3** presented interesting inhibition. Again it was observed that the transformation to a *bis*-chalcone with an ether linkage led to more potent analogues with more potent representatives the **a2–b3/b2–b3**.

Perusal of *Clog P* and IC₅₀ or %AChE values in Tables 1 and 2 revealed that the role of lipophilicity on the inhibition of AChE was not well defined in this series of compounds.

Figure 3. Inhibition % of AChE induced by 100 μ M of compounds **a3**, **b** (2–4) in relation to the time (0–30 min).

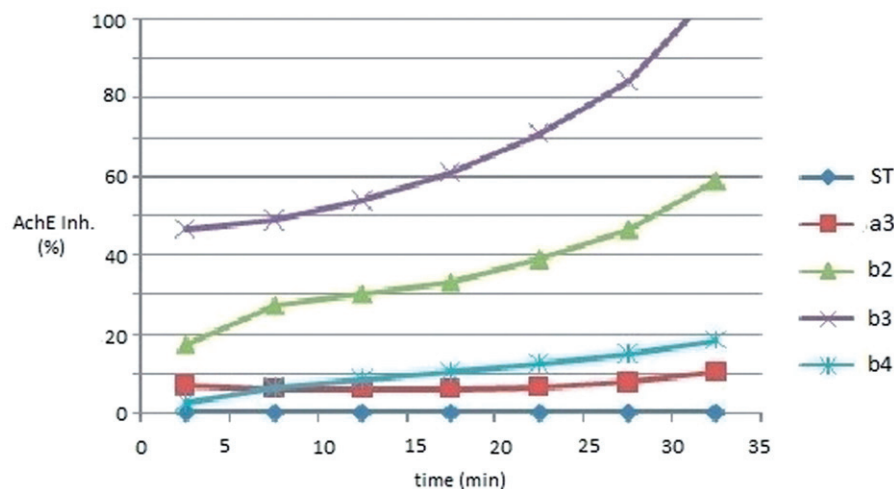


Table 4. Stability studies and incubation with GSH.

α/α	λ_{nm} (max)	ϵ_{max}
a1	340	2200
a1 + 2GSH	340	1800
a2	256	14 200
a2 + 2GSH	256	8600
a3	326	2700
a3 + 2GSH	326	5000
a4	326	11 500
a4 + 2GSH	326	15 500
c	245	0
c + 2GSH	245	600
b1	246	1500
b1 + 2GSH	246	1500
b2	341	12 700
b2 + 2GSH	341	3700
b3	320	9900
b3 + 2GSH	320	0
b4	443	12 460
b4 + 2GSH	443	0

Analyzing this data set as a wholesome, lipophilicity did not seem to affect absolutely the AChE inhibition. Within the **a1**–**b4** subgroup lower *clog P* values (**a3** = 3.66) were correlated to higher activity. This concept was not followed by *bis*-chalcones.

To further investigate the inhibition mechanism, time dependence of AChE inhibition by compounds **a3**, **b2**, **b3** and **b4** was subsequently probed. For the time 0–30 min the data showed a continued increase (Figure 3). The inhibition seems to be time dependent.

Glutathione (GSH) conjugation constitutes an *in vivo* antioxidant protective mechanism, by which reactive electrophilic compounds are detoxified by virtue of its nucleophilic sulphhydryl group. The nucleophilic addition of GSH to electron-deficient carbon double bonds occurs mainly in compounds with α,β -unsaturated double bonds like chalcones demonstrating preferential reactivity toward thiols in contrast to amino and hydroxyl groups²⁷. In our case, we have studied the possibility of alkylation of our *mono/bis-chalcones* with a cellular thiol such as GSH, leading to the adducts A. In most instances the double bond was rendered electron deficient by resonance or conjugation with the carbonyl group.

It should be emphasized that chalcones **a1**, **a2** and **b2** were conjugated with 2 GSH, **a4** presented slight alkylation rate

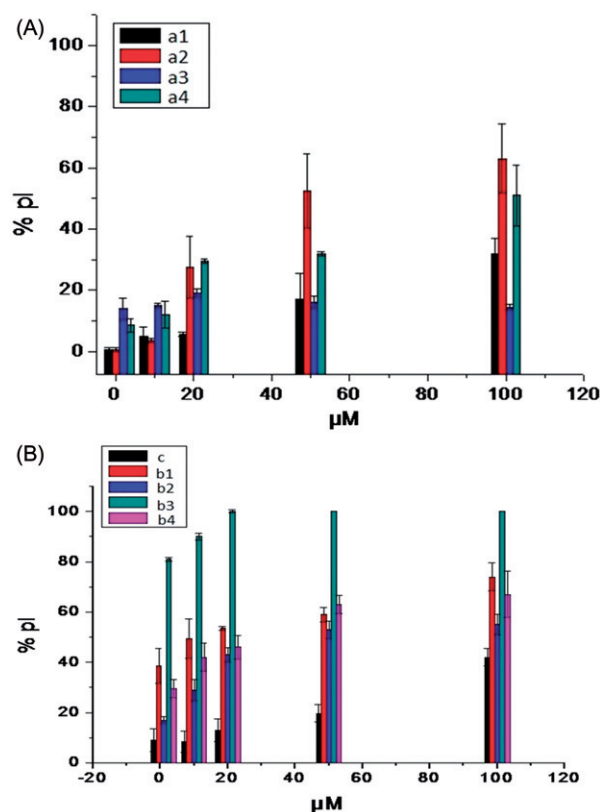
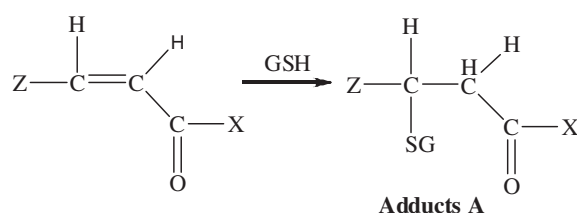


Figure 4. Cytotoxicity of chalcones (**a1**–**a4**) and *Bis*-chalcones–ethers (**b1**–**b4**) on L929 cells (24-h incubation) expressed as PI % values.

whereas *bis*-**b3** and **b4** were highly conjugated with GSH (Table 4). The others, e.g. **a3** and **b1** did not exhibit any interaction. It seems that the stereochemistry of substituent Z affects the alkylation.



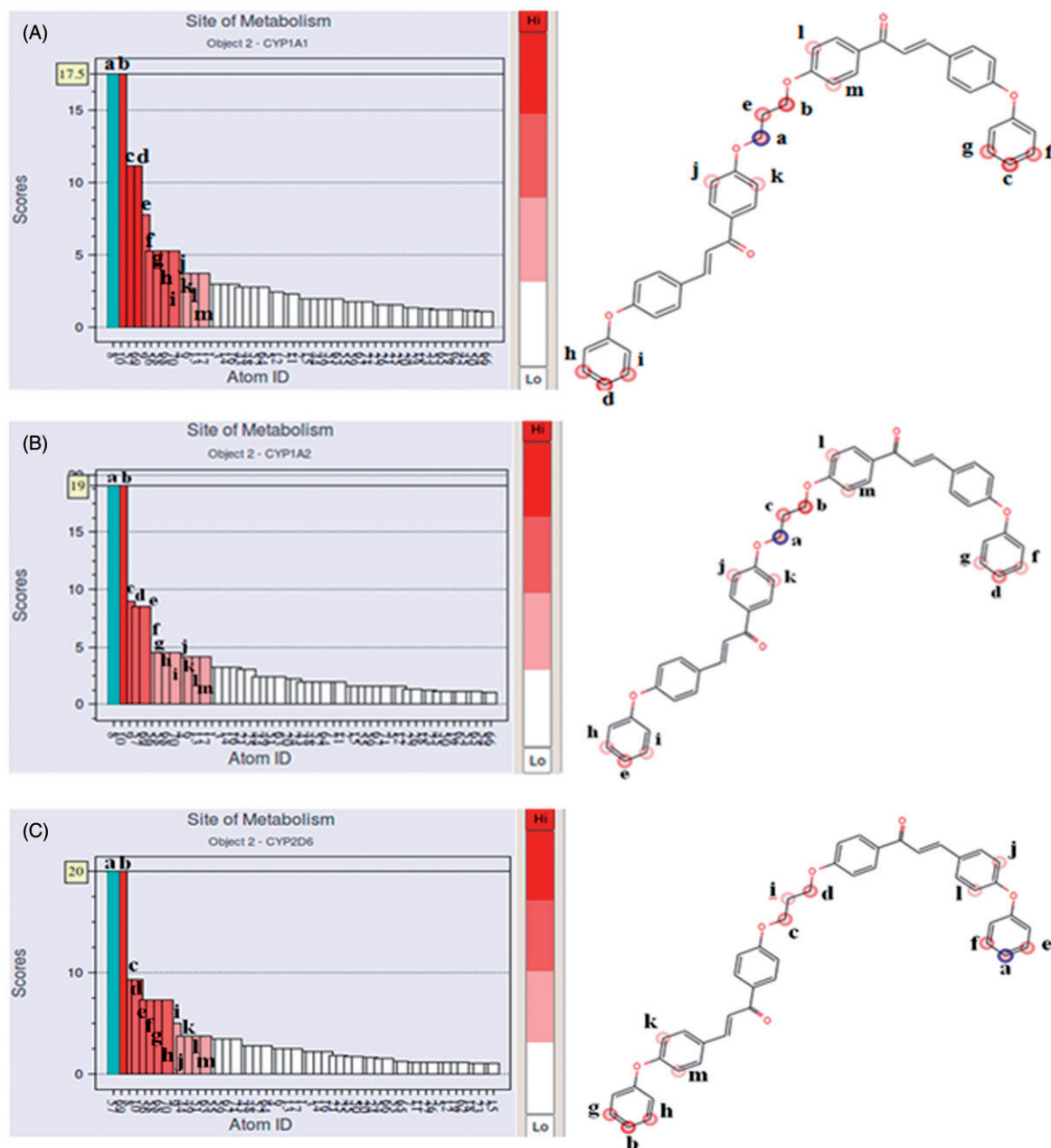


Figure 5. Histogram (left) and graphical visualization (right) of predicted (A) CYP1A1, (B) CYP1A2, (C) CYP2D6 metabolic sites for compound **b2**. Four different shades of color are used; from dark (lowest probability) to white (highest). The major metabolic site is highlighted (blue color).

Cytotoxicity

The cytotoxicity of the synthesized derivatives was determined using the PI fluorescence method^{35,42} in the presence of different concentrations (1–100 μ M) of these compounds.

The results are presented in Figure 4 in the form a bar-graph of the % cell survival values as PI % values for the examined compounds. All tested chalcones **a** (**1–4**) showed low cytotoxicities in the whole area of concentrations examined (from 1 to 100 μ M), with the noticeable exception of **a2** and **a4**. Considering the *bis*-chalcone ethers, **b3** was found to present high toxicity started at the concentration of 1 μ M (81%) reaching the highest values at 20 μ M (100%). The rest *bis*-derivatives follow, with the exception of **b2** whose toxicity started increasing significantly at the concentration of 20 μ M reaching the highest values at 100 μ M (55%).

Molecular docking studies

Prediction of the site of metabolism by CYP1A1, CYP1A2 and CYP2D6

CYP family is one of the important steroid-metabolizing enzymes. In general, metabolic transformations tend to reduce the bioavailability of a compound and, in turn, the pharmacological profile. Therefore, we have computed the prediction of the site of metabolism using the MetaSite software (version 5.0.3, Molecular Discovery Ltd., 2014; www.moldiscovery.com). MetaSite can be used to evaluate the metabolic stability from the 3D structure of a drug candidate prior to experimental measurements. Three CYP enzyme isoform CYP1A1, CYP1A2 and CYP2D6 were selected for the prediction of the site of metabolism for compound **b2**. Figure 5 reports the histogram with the PSM values (Site of Metabolism

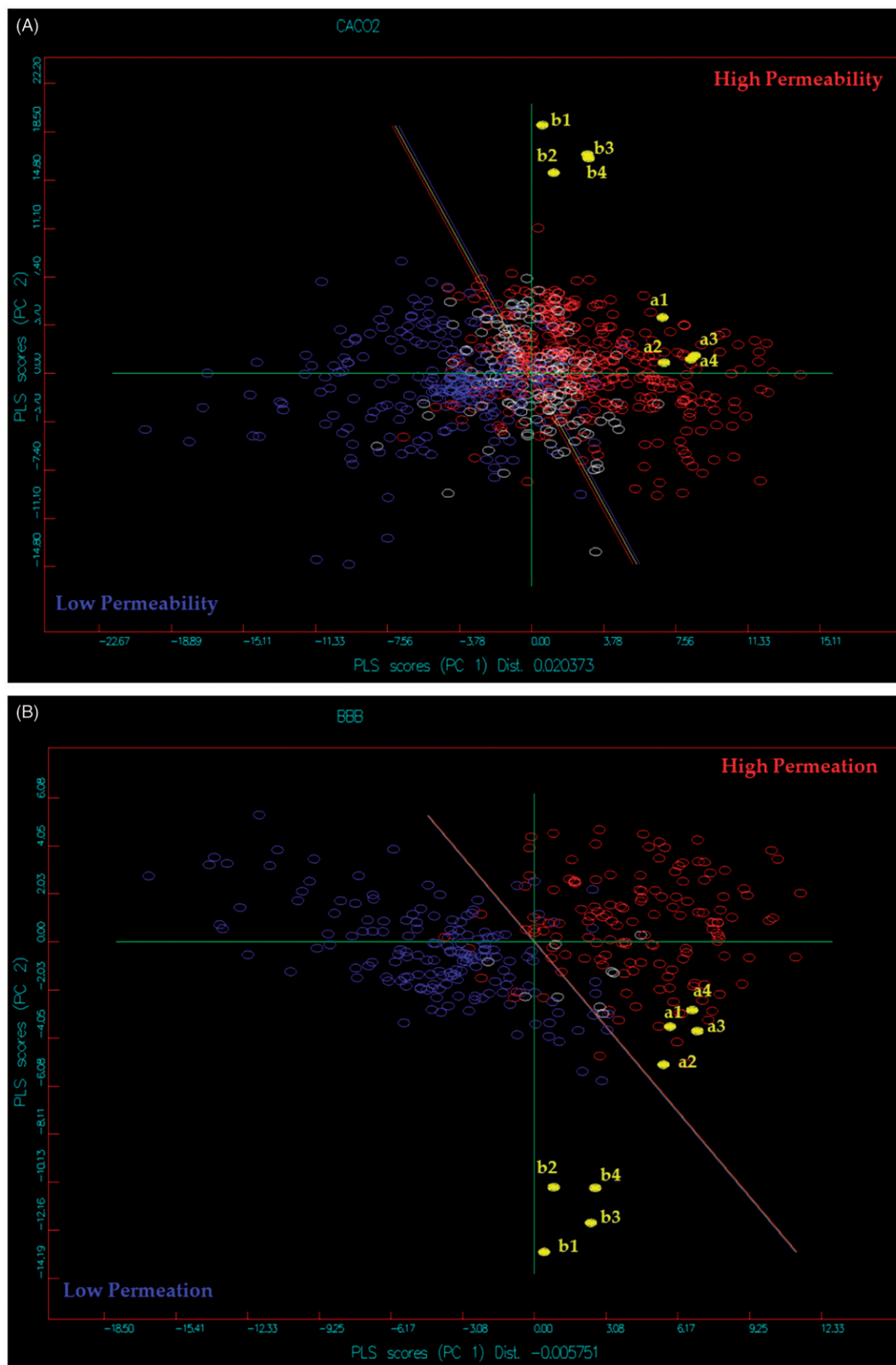


Figure 6. *In silico*: (A) Caco-2 permeability and (B) BBB permeation.

Probability), for each of the substrate atoms considered in the computation by the three enzymes. It is observed that the most probable sites of metabolism for the enzymes CYP1A1 and CYP1A2 are the hydrogens of the $-\text{OCH}_2\text{CH}_2\text{CH}_2\text{O}-$ linkage, while for the enzyme CYP2D6 the most probable site of metabolism are the para-hydrogens of the two O-benzyl groups.

In silico Caco-2 permeability and BBB permeation

The compounds were projected on the precalculated models of VolSurf: Caco-2 cell absorption and BBB passage. Regarding to the Caco-2 cell permeability, the 2D partial least squares (PLS) score model can discriminate between permeable and less

permeable compounds. When the spectrum color is active, red points refer to high permeability and blue points refer to low permeability. The PLS score space of the BBB model is divided into, (i) a region (left) in which BBB ranges from negative values up to -0.3 , this is the region in which compounds show no ability to cross the BBB, (ii) a small region (central) for BBB values from -0.3 to $+0.3$ (in between red and blue lines) where compounds show moderate permeability and (iii) a region (right) in which BBB values ≥ 0.3 are found, this is the region in which compounds show ability to cross the BBB.

It is observed from the two plots that simple chalcones, the compounds **a1–a4** are located in the region of high permeability and therefore they can be transported across the intestinal epithelium cross (Figure 6) and they can across the BBB. The *bis*-chalcones, compounds **b1–b4** are located in the region of low permeation on the BBB plot and high permeability on the Caco-2 plot. However, it should be taken into consideration that these compounds cover an empty chemical space and the prediction for these molecules could be doubtful.

Conclusions

In conclusion, **a** and **b** chalcones represent promising class of antioxidant and anti-LOX enones with anti-AChE activities. These results lead us to propose **b2** and **b3** as new multifunctional compounds against AD. The α,β -unsaturated ketone moiety is considered the key pharmacophore feature. The presence of a double enone group supports better biological results, whereas the rest structural element seems to quantitatively offer to the activity.

The pharmacokinetic findings seem quite interesting and useful to the design and optimization of the pharmacokinetic profile of new derivatives. As the most probable sites of metabolism for the enzymes CYP1A1 and CYP1A2 are the hydrogens of the $-\text{CH}_2\text{CH}_2\text{CH}_2\text{O}-$ linkage, it seems possible that the molecules of the **b** group to act as prodrugs. Further investigation is in progress to study this possibility.

Mechanistic studies attempting to determine the actual mode of the antioxidative, anti-LOX and anti-AChE action and most derivatives are under way. In addition, application of the present methodology to the preparation of further examples of *bis*-chalcones with different ether chains, suitable for structure–activity relationship studies, as well as attaching medicinally interesting molecules on the **b** constructs (**b2** and **b3**), and the biological evaluation of the synthesized compounds in other cellular targets, are currently in progress.

Acknowledgements

We would like to thank Dr A. Leo and Biobyte Corp., 201 West 4th Str., Suite 204, Claremont, CA 91711, USA for free access to the C-QSAR program. We are also grateful to Prof. Gabriele Cruciani (Laboratory of Chemoinformatics and Molecular Modeling, School of Chemistry, University of Perugia, Italy) for kindly providing us the MetaSite and Volsurf programs.

Declaration of interest

The authors report no conflicts of interest.

References

- Hasan A, Khan KM, Sher M, et al. Synthesis and inhibitory potential towards acetylcholinesterase, butyrylcholinesterase and lipoxigenase of some variably substituted chalcones. *J Enzyme Inhib Med Chem* 2005;20:41–7.
- Katsori AM, Hadjipavlou-Litina D. Recent progress in therapeutic applications of chalcones. *Exp Opin Ther Patents* 2011;10:1575–96.
- Maurya DK, Devasagayam TP. Antioxidant and prooxidant nature of hydroxycinnamic acid derivatives ferulic and caffeic acid. *Food Chem Toxicol* 2010;48:3369–73.
- Ka MH, Choi EH, Chun HS, Lee KG. Antioxidative activity of volatile extracts isolated from *Angelica tenuissimae* roots, peppermint leaves, pine needles and sweet flag leaves. *J Agric Food Chem* 2005;53:4124–9.
- Molina-Jimenez MF, Sanchez-Reus MI, Andres D, et al. Neuroprotective effect of fraxetin and myricatin against rotenone-induced apoptosis in neuroblastoma cells. *Brain Res* 2004;1009:9–16.
- Labieniec M, Gabryelak T. Study of interactions between phenolic compounds and H_2O_2 or Cu(II) ions in B14 Chinese hamster cells. *Cell Biol Intern* 2006;30:761–8.
- McGeer EG, McGeer PL. Inflammatory processes in Alzheimer's disease. *Progr Neuro-Physiopharm Biol Psych* 2003;27:741–9.
- Garcia-Ayllon MS, Small DH, Avila J, Saez-Valero J. Revisiting the role of acetylcholinesterase in Alzheimer's disease: cross-talk with P-tau and β -amyloid. *Front Mol Neurosci* 2011;22:1–9.
- Francis PT, Palmer AM, Snape M, Wilcock GKJ. The cholinergic hypothesis of Alzheimer's disease: a review of progress. *Neuro Neurosurg Psychiatry* 1999;66:137–47.
- Crooks SW, Stockley RA. Leukotriene B4. *Int J Biochem Cell Biol* 1998;30:173–8.
- Praticò D. Oxidative stress hypothesis in Alzheimer's disease: a reappraisal. *Trends Pharmacol Sci* 2008;29:609–15.
- Firuzi O, Zhuo J, Chinnici CM, et al. 5-Lipoxygenase gene disruption reduces amyloid- β pathology in a mouse model of Alzheimer's disease. *FASEB J* 2008;22:1169–78.
- Chu J, Li JG, Ceballos-Diaz C, et al. The influence of 5-lipoxygenase on Alzheimer's disease-related tau pathology: *in vivo* and *in vitro* evidence. *Biol Psychiatry* 2013;74:321–8.
- Brown D, Superti-Furga G. Rediscovering the sweet spot in drug discovery. *Drug Discov Today* 2003;8:1067–77.
- Szuromi P, Vinson V, Marshall E. Rethinking drug discovery. *Introduction. Science* 2004;303:1795–9.
- Overington JP, Al-Lazikani B, Hopkins AL. Opinion. How many drug targets are there? *Nat Rev Drug Discov* 2006;5:993–9.
- Mahreen A, Sugunadevi S, Guang Ping G, Keun WL. An innovative strategy for dual inhibitor design and its application in dual inhibition of human thymidylate synthase and dihydrofolate reductase enzymes. *PLoS One* 2013;8:e60470.
- Csermely P, Agoston V, Pongor S. The efficiency of multi-target drugs: the network approach might help drug design. *Trends Pharmacol Sci* 2005;26:178–82.
- Cruciani G, Pastor M, Guba W. VolSurf: a new tool for the pharmacokinetic optimization of lead compounds. *Eur J Pharm Sci* 2000;11:29–39.
- Ravi VM, Vidya J. Synthesis and insecticidal activity of new substituted phenoxychalcones. *Indian J Chem* 1995;34:56–457.
- Vanangamudi G, Thirunarayanan G. Effects of substituents on IR deformation modes of vinyl system in 1-naphthyl ketones. *Int J Chem Sci* 2006;4:787–90.
- Sodani RS, Choudhary PC, Sharma HO, Verma BL. Syntheses and reactions of 4'-[(w-Bromoalkyl)oxy]- and 4',4''-(Polymethylenedioxy)-*bis* substituted chalcones. *Eur J Chem* 2010;7:763–9.
- Rekker R. The hydrophobic fragmental constant. Its derivation and application. A means of characterizing membrane systems. The Netherlands: Elsevier Eds Scientific Co.; 1977:1.
- Biobyte Corp. C-QSAR Database 201. Claremont, CA. Available from: www.biobyte.com [last accessed June 2014].
- Pontiki E, D. Hadjipavlou-Litina D. Synthesis and pharmacochemical evaluation of novel aryl-acetic acid inhibitors of lipoxigenase, antioxidants, and anti-inflammatory agents. *Bioorg Med Chem* 2007;15:5819–27.
- Liégeois C, Lermusieau G, Collins SJ. Reducing powers of various hop varieties. *Agric Food Chem* 2000;48:1129–34.
- Dimmock JR, Kandepu NM, Hetherington M, et al. Cytotoxic activities of Mannich bases of chalcones and related compounds. *J Med Chem* 1998;41:1014–26.
- Ellman GL, Courtney KD, Andres V, Featherstone RM. A new and rapid colorimetric determination of acetylcholinesterase activity. *Biochem Pharm* 1961;7:88–95.
- Sybyl. Version 8.0. St. Louis, MO: TRIPOS Associates Inc.; 2008.
- Vinter JG, Davis A, Saunders MR. Strategic approaches to drug design. I. An integrated software framework for molecular modeling. *J Comput Aided Mol* 1987;1:31–51.

31. Boyer S, Zamora I. New methods in predicting metabolism. *J Comput Aided Mol* 2002;16:403–13.
32. Zamora I, Afzelius L, Cruciani G. Predicting drug metabolism: a site of metabolism prediction tool applied to the cytochrome P450 2C9. *J Med Chem* 2003;46:2313–24.
33. Crivori P, Cruciani G, Carrupt PA, Testa B. Predicting blood–brain barrier permeation from three-dimensional molecular structure. *J Med Chem* 2000;43:2204–16.
34. Cruciani G, Crivori P, Carrupt PA, Testa B. Molecular fields in quantitative structure–permeation relationships: the VolSurf approach. *J Mol Struct Theochem* 2000;503:17–30.
35. Dengler WA, Schulte J, Berger DP, et al. Development of a propidium iodide fluorescence assay for proliferation and cytotoxicity assays. *Anti-Cancer Drugs* 1995;6:522–32.
36. Kulisic T, Radonic A, Katalinic V, Milos M. Use of different methods for testing antioxidative activity of oregano essential oil. *Food Chem* 2004;85:633–40.
37. Koleva II, Van Beek TA, Linssen JPH, et al. Screening of plant extracts for antioxidant activity: a comparative study on three testing methods. *Phytochem Anal* 2001;13:8–17.
38. Huang D, Ou B, Prior RL. The chemistry behind antioxidant capacity assays. *J Agric Food Chem* 2005;53:1841–56.
39. Taraborewala RB, Kauffman JM. Synthesis and structure activity relationships of anti-inflammatory 9,10-dihydro-9-oxo-2-acridine – alkanolic acids and 4-(2-carboxyphenyl)aminobenzene alkanolic acids. *J Pharm Sci* 1990;79:173–8.
40. Pontiki E, Hadjipavlou-Litina D. Lipxygenase inhibitors: a comparative QSAR study review and evaluation of new QSARs. *Med Res Rev* 2008;28:39–117.
41. Kang JE, Cho JK, Marcus J, et al. Inhibitory evaluation of sulfonamide chalcones on β -secretase and acylcholinesterase. *Park Mol* 2013;18:140–53.
42. Benvenuto JA, Connor TH, Monteith DK, et al. Degradation and inactivation of antitumor drugs. *J Pharm Sci* 1993;82:988–91.